

## Selective Aggregation of Single-Walled Carbon Nanotubes via Salt Addition

Sandip Niyogi,<sup>†</sup> Sofiane Boukhalfa,<sup>†</sup> Satishkumar B. Chikkannanavar,<sup>†</sup> Timothy J. McDonald,<sup>‡</sup> Michael J. Heben,<sup>‡</sup> and Stephen K. Doorn<sup>\*†</sup>

Chemistry Division, Los Alamos National Laboratory, C-CSE, Los Alamos, New Mexico 87545, and Center for Basic Sciences, National Renewable Energy Laboratory, Golden, Colorado 80401

Received November 28, 2006; E-mail: skdoorn@lanl.gov

Single-walled carbon nanotubes (SWNTs) can be dispersed as individuals in H<sub>2</sub>O using sodium dodecylsulfate (SDS), typically at 1% (35 mM) concentration. At and above the critical micellar concentration (cmc 8 mM at 25 °C), the degree of ionization of SDS is 0.27.<sup>1</sup> Once intertube van der Waals (VdW) attraction is overcome by intense sonication, free SDS adsorbs to SWNT surfaces and creates a net surface density of negative charge, which prevents SWNT reaggregation. In such solutions, the excitonic absorption and emission of light by the various SWNT chiralities can be observed.<sup>2–4</sup> Any change in the surface charge density of the surfactant, or its solubility, that eliminates the electrostatic repulsion between the nanotubes will cause SWNTs to aggregate and coagulate.<sup>4</sup>

By controlling the intermolecular and surface forces of SDS in water, we show here that it is possible to engineer the resultant VdW attraction between SWNTs. Titrating SWNT–SDS dispersions with salt solutions leads to diameter-dependent modulation of the electrostatic repulsive forces; changes in the absorbance and emission spectra of SWNTs are used to study these effects. We ascribe the observed spectroscopic changes to selective aggregation of SWNT chiralities. Our experiments clearly demonstrate that certain SWNT chiralities deviate from a simple diameter-dependent stability trend.

A 20.0 mg quantity of as-prepared HiPco SWNTs was dispersed in 200 mL of 35 mM SDS (Fisher, 98%) in D<sub>2</sub>O (4.4 × cmc), using the standard procedure of shear mixing and sonication followed by ultracentrifugation.<sup>2</sup> Microliter volumes of salt solutions (~1 M in D<sub>2</sub>O) were added to the SWNT dispersions at room temperature. The experiments were reproduced in up to 10 mL of the SWNT dispersions. Aliquots were taken out to record the spectra. After salt addition, the solutions were either stirred or allowed to stand overnight to attain equilibrium. Absorbance spectra were recorded in a Varian Cary 6000i instrument. Excitation maps of the SWNT photoluminescence were recorded using a home-built FT-photoluminescence excitation (PLE) spectrometer with a Xe arc lamp source and a liquid N<sub>2</sub>-cooled Ge detector from a modified Nicolet NXR-9600 FT-IR spectrometer.<sup>5</sup> Excitation power at the sample was typically 1.3 mW, and the emission spectra were integrated over 128 scans. The single line ( $\lambda_{\text{EX}} = 780 \text{ nm}$ ) emission spectra (Figure 1) were recorded using the same Nicolet spectrometer with diode laser excitation.

Systematic changes in the emission features are observed as NaCl is added to the SWNT dispersion (Figure 1). With respect to the starting SWNT dispersion (Figure 1A), in 0.14 M NaCl, the background is suppressed and the emission intensity is enhanced, particularly for the larger-diameter SWNTs (Figure 1B). As the concentration of NaCl is increased, the emission from certain SWNT chiralities is no longer observed. It is particularly interesting to note

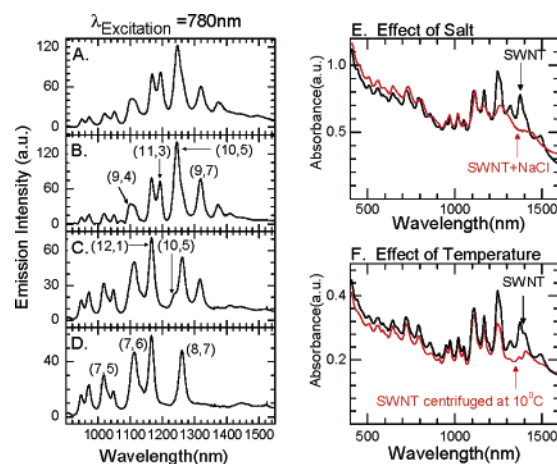


**Figure 1.** Spectroscopy of SWNT–SDS dispersions as a function of salt concentration and temperature. (A) emission spectrum of the starting SWNT–SDS dispersion; (B) same solution in 0.14 M NaCl; (C) in 0.43 M NaCl, and (D) in 0.57 M NaCl; (E) absorption spectrum with and without NaCl (0.17 M); (F) change in the absorption spectrum at temperatures below the critical micellar temperature.

that in the band corresponding to the (10,5) and (8,7) emissions, the (10,5) emission is no longer visible in 0.43 M NaCl (Figure 1C); similarly, (11,3) and (9,4) signals are absent. The emission intensity of (7,5) and (6,5) chiralities increase, under the same conditions. In 0.57 M NaCl, the (9,7) emission is also completely lost (Figure 1D).

The cmc of pure SDS is reduced to 1 mM in 0.16 M NaCl.<sup>6</sup> The addition of Na<sup>+</sup> decreases the electrostatic repulsion between SDS molecules and results in an increase in their aggregation number. Since we also observe that the completely aggregated dispersions show the background-only emission spectrum, the increase in the emission intensity and loss of the background emission (Figure 1B) may be due to improved isolation of the SWNTs, related to the ionization degree and aggregation number of SDS under these conditions (see also Supporting Information, Figure S2).<sup>6,7</sup> Above 0.5 M NaCl, pure SDS is no longer soluble in water at 25 °C;<sup>8</sup> under these conditions, the Kraft point of pure SDS is raised above 25 °C.<sup>9</sup> The Kraft point is the melting point of a hydrated surfactant; it is raised by the addition of salt in water. We expect the concentration of NaCl necessary to affect the stability of SWNT/SDS dispersions to be different from values previously obtained for pure SDS solutions. However, lowering the dispersion temperature should yield an effect similar to elevating the Kraft point. We observe a diameter-dependent change in the absorbance spectrum on centrifuging the SWNT dispersion at 70000g for 3 h, at 10 °C (Figure 1F), similar to the effect of adding NaCl (Figure 1E).

Thus, manipulation of SDS equilibria results in loss of free SDS in solution, through precipitation or further micellization. SWNT–

<sup>†</sup> Los Alamos National Laboratory.

<sup>‡</sup> Center for Basic Sciences, National Renewable Energy Laboratory.

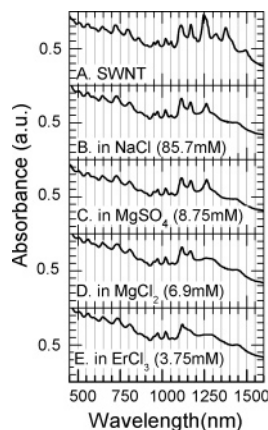


**Figure 2.** Absorption spectra of SWNTs showing the chirality-dependent aggregation and broadening in the presence of salts of varying counterion valency and ionic strengths.

bound SDS is lost in response, resulting in nanotube aggregation as electrostatic repulsion is reduced. That large-diameter tubes are observed to selectively aggregate first in these experiments is likely a consequence of a progressively increasing stability of SDS binding to smaller-diameter SWNTs.<sup>10</sup> Addition of salt at constant SDS concentration allows us to observe the intermediate equilibria where certain SWNT chiralities exhibit enhanced stability with respect to aggregation, when compared to chiralities of similar diameter. Specifically, as seen in Figure 1B–D, the (12,1), (9,7), and (8,7) chiralities do not aggregate (see Supporting Information), while spectral features from similar diameter SWNTs are lost. Chirality specific SWNT–surfactant interactions may be responsible for this additional stability.

Charge screening effects can also reduce intertube repulsion. The SWNT–SDS system can be considered to be a negative surface of  $\text{SO}_4^-$  with  $\text{Na}^+$  counterions. The density of the  $\text{SO}_4^-$  groups determines the surface potential of the SWNTs, which in turn would determine the separation between adjacent SWNTs. If the ionic concentration of the counterion is increased, the surface can be completely neutralized, at which point the adjacent SWNTs would come into contact due to van der Waals attraction.<sup>11</sup> The concentration of counterions necessary to completely neutralize the surface charge decreases significantly for divalent or trivalent cations, due to better charge screening.<sup>11</sup>

In Figure 2, we show the effect of di- and trivalent counterions on the absorbance spectrum of SWNTs. In general, the spectra show a progressive shift in the stability of SWNT chiralities toward narrower diameters as the valency of the cation is increased (Figure 2B, D, and E). In Figure 2C and D, we compare the effect of ionic strength of the added salt on the stability of SWNT chiralities. Clearly,  $\text{MgCl}_2$  is relatively more efficient in aggregating SWNT chiralities. Since the reactions are allowed to reach equilibrium, these results indicate that initial surface charge densities are lower for larger-diameter SWNTs.

The emission spectrum of SWNTs is more sensitive to the internanotube distances. The change in the emission spectrum of the SWNT solutions is shown in Figure 3. The PLE map of the starting SWNT solution shows 14 SWNT chiralities distinctly (Figure 3A). All chiralities present in the HiPco sample within the limits of our excitation range are labeled. The loss of the absorption peaks in Figure 2 is concurrent with the absence of the corresponding emission bands.

Thus, fine control over the SWNT aggregation state is possible with salt additions, which result in selective aggregation of a very narrow-diameter range. This behavior suggests that, at any particular

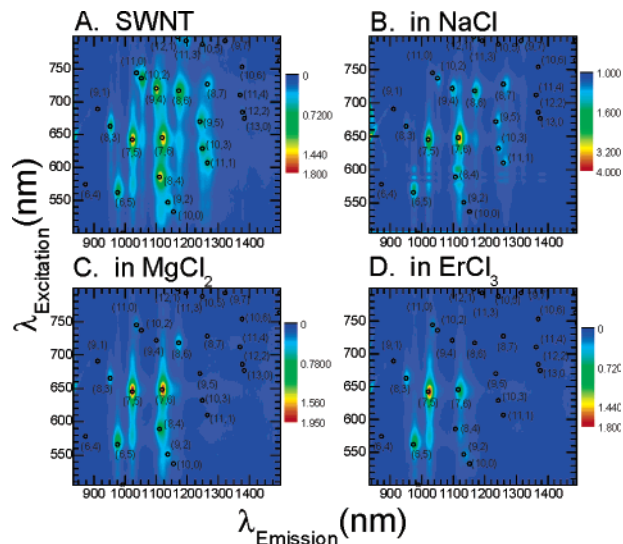


**Figure 3.** Contour plots of SWNT photoluminescence with excitation from 500 to 800 nm at 5 nm intervals. Each bright spot corresponds to a SWNT chirality as labeled. (A) The starting SWNT dispersion; (B) SWNTs in 57.5 mM NaCl; (C) SWNTs in 6.9 mM  $\text{MgCl}_2$ ; (D) SWNTs in 3.75 mM  $\text{ErCl}_3$ .

concentration of salt being added, SWNTs of identical chiralities may self aggregate. Manipulating surfactant equilibria in the manner demonstrated above shows significant promise toward separation of SWNTs by diameter and crystallization of pure chiralities. Isolation of the aggregates in analytically pure form will require optimization of the stability of the aggregates, over the various vectors such as solution temperature and the nature of the counterion, as we identify in this work.

**Acknowledgment.** We thank Brian Fishbine and Cris Lewis for help with setting up the FT-PLS system. This work was supported by LANL LDRD funding. T.J.M. and M.J.H. were supported by the U.S. Department of Energy, Office of Science, Solar Photochemistry Research Program.

**Supporting Information Available:** Chirality specific emission intensity vs SWNT diameter analysis for Figure 1A–D. This material is available free of charge via the Internet at <http://pubs.acs.org>.

## References

- Bales, B. L. *J. Phys. Chem. B* **2001**, *105*, 6798.
- O'Connell, M. J.; Bachilo, S. M.; Huffman, C. B.; Moore, V. C.; Strano, M. S.; Haroz, E. H.; Rialon, K. L.; Boul, P. J.; Noon, W. H.; Kittrell, C.; Ma, J.; Hauge, R. H.; Weisman, B. R.; Smalley, R. E. *Science* **2002**, *297*, 593.
- Bachilo, S. M.; Strano, M. S.; Kittrell, C.; Hauge, R. H.; Smalley, R. E.; Weisman, B. R. *Science* **2002**, *298*, 2361.
- Tan, Y.; Resasco, D. E. *J. Phys. Chem. B* **2005**, *109*, 14454.
- McDonald, T. J.; Jones, M.; Engtrakul, C.; Ellingson, R. J.; Rumbles, G.; Heben, M. J. *Rev. Sci. Instrum.* **2006**, *77*, 053104.
- Wanless, E. J.; Ducker, W. A. *J. Phys. Chem. B* **1996**, *100*, 3207.
- Benrraou, M.; Bales, B. L.; Zana, R. *J. Phys. Chem. B* **2003**, *107*, 13432.
- Hayashi, S.; Ikeda, S. *J. Phys. Chem. B* **1980**, *84*, 744.
- Nakayama, H.; Shinoda, K. *Bull. Chem. Soc. Jpn.* **1967**, *40*, 1797.
- McDonald, T. J.; Engtrakul, C.; Jones, M.; Rumbles, G.; Heben, M. J. *J. Phys. Chem. B* **2006**, *110*, 25339.
- Israelachvili, J. N. *Intermolecular and Surface Forces*; Academic Press: San Diego, 1985.

JA068321J